EJN European Journal of Neuroscience

FENS Federation of European Neuroscience Societies

European Journal of Neuroscience, pp. 1–9, 2016 doi:10.1111/ejn.13278

Insulin-like growth factor-I gene therapy increases hippocampal neurogenesis, astrocyte branching and improves spatial memory in female aging rats

Joaquín Pardo,[1,2] Maia Uriarte,[1,2] Gloria M. Cónsole,[2] Paula C. Reggiani,[1,2] Tiago F. Outeiro,[3] Gustavo R. Morel[1,2,a] and Rodolfo G. Goya[1,2,a]

[1]INIBIOLP-Pathology B, School of Medicine, UNLP, CC 455, 1900 La Plata, Argentina

[2]Department of Histology and of Embryology B, School of Medicine, UNLP, La Plata, Argentina

[3]Department of Neurodegeneration and Restorative Research, Center for Nanoscale Microscopy and Molecular Physiology of the Brain, University Medical Center Göttingen, Göttingen, Germany

Keywords: aging, Barnes maze, gene therapy, hippocampal morphology, IGF-I, spatial memory

Edited by Thomas Klausberger

Received 9 March 2016, revised 24 April 2016, accepted 10 May 2016

Abstract

In rats, learning and memory performance decline during aging, which makes this rodent species a suitable model to evaluate therapeutic strategies of potential value for correcting age-related cognitive deficits. Some of these strategies involve neurotrophic factors like insulin-like growth factor-I (IGF-I), a powerful neuroprotective molecule in the brain. Here, we implemented 18-day long intracerebroventricular (ICV) IGF-I gene therapy in 28 months old Sprague–Dawley female rats, and assessed spatial memory performance in the Barnes maze. We also studied hippocampal morphology using an unbiased stereological approach. Adenovectors expressing the gene for rat IGF-I or the reporter DsRed were used. Cerebrospinal fluid (CSF) samples were taken and IGF-I levels determined by radioimmunoassay. At the end of the study, IGF-I levels in the CSF were significantly higher in the experimental group than in the DsRed controls. After treatment, the IGF-I group showed a significant improvement in spatial memory accuracy as compared with DsRed counterparts. In the dentate gyrus (DG) of the hippocampus, the IGF-I group showed a higher number of immature neurons than the DsRed controls. The treatment increased hippocampal astrocyte branching and reduced their number in the hippocampal stratum radiatum. We conclude that the ependymal route is an effective approach to increase CSF levels of IGF-I and that this strategy improves the accuracy of spatial memory in aging rats. The favorable effect of the treatment on DG neurogenesis and astrocyte branching in the stratum radiatum may contribute to improving memory performance in aging rats.

Introduction

Cognitive aging and its most devastating expression, Alzheimer's disease (AD), represent a growing medical and socioeconomic challenge that calls for vigorous research efforts across the globe to design effective therapeutic interventions (Ravindranath *et al.*, 2015). In humans and rats, brain aging is associated with a progressive deterioration of spatial learning and memory, which makes this rodent species a suitable model to evaluate therapeutic strategies of potential value for correcting age-related cognitive deficits. Some of these strategies involve the administration of neurotrophic factors, one of which, insulin-like growth factor-I (IGF-I), is emerging as a promising molecule that plays a physiologic role in neuroprotection. Thus, IGF-I is known to be induced in the central nervous system (CNS) after ischemia (Beilharz *et al.*, 1998), neocortical lesions (Walter *et al.*, 1997; Li *et al.*, 1998) and spinal cord injury (Yao *et al.*, 1995). Cytotoxic damage to the hippocampus is associated with a large increase in the production of IGF-I and IGF-I binding protein 2, by the microglia, a finding that suggests a neuroprotective role of IGF-I in the brain (Breese *et al.*, 1996). Intracerebroventricular (ICV) infusion of IGF-I in the lateral ventricle improves reference and working memory in aging rats (Markowska *et al.*, 1998). Also, it has been documented that IGF-I protects hippocampal neurons from the toxic effects of amyloid peptides (Dore *et al.*, 1997). Furthermore, IGF-I treatment markedly reduced the brain burden of Aβ amyloid in transgenic mice carrying a mutant Aβ amyloid peptide (Carro *et al.*, 2006a).

Gene therapy for IGF-I in the CNS of senile rats has shown promising results. Thus, an adenoviral vector harboring the gene for IGF-I was used to implement IGF-I gene therapy in the hypothalamus of aging female rats displaying tuberoinfundibular dopaminergic neurodegeneration and chronic hyperprolactinemia. The

Correspondence: Rodolfo Goya, as above.
E-mail: goya@isis.unlp.edu.ar

[a]These two authors contributed equally to this study.

treatment reversed the hyperprolactinemia and increased the number of dopaminergic neurons in the hypothalamus of the aging rats (Hereñú *et al.*, 2007). Hypothalamic IGF-I gene therapy in middle-aged female rats significantly prolonged their regular estrous cyclicity and preserved ovarian structure when compared with placebo-treated females (Rodriguez *et al.*, 2013). As the ependymal route is particularly suitable for RAd-mediated gene delivery, it can effectively increase IGF-I levels in the cerebrospinal fluid (CSF) of rats (Hereñú *et al.*, 2009). Taking advantage of this fact, we performed ICV IGF-I gene therapy in very old female rats and achieved a significant amelioration of their motor performance (Nishida *et al.*, 2011).

The above facts prompted us to assess the restorative ability of ICV IGF-I gene delivery on spatial memory performance in old female rats. A set of hippocampal cell markers was also quantitated in the animals by means of an unbiased stereological approach.

Materials and methods

Adenoviral vectors

RAd-IGF-I

A recombinant adenoviral (RAd) vector harboring the gene for rat IGF-I (provided by Peter Rotwein, Oregon Health Sciences University) was constructed by a previously described procedure (Hereñú *et al.*, 2007). The cDNA of rIGF-I was placed under the control of the mouse cytomegalovirus (mCMV) promoter. The new adenovector was rescued from HEK293 cell lysates and plaque purified. It was further purified by ultracentrifugation in a CsCl gradient. Final adenoviral stock was titrated using a serial dilution plaque assay.

RAd-(DsRed)

This adenovector was constructed according to the general procedures outlined above. The vector expresses the gene for the *Discosoma* sp. red fluorescent protein DsRed2, driven by the mCMV promoter. The vector was expanded in 293 cells and purified and titrated as described above.

Animals

Twenty-two 28-month-old female Sprague–Dawley (SD) rats raised in our Institution's animal facilities (INIBIOLP) were used. Twenty animals were randomly divided into two groups, ten animals each: Group IGF-I, which received RAd-IGF-I at the time of vector injection and group DsRed, which received the DsRed adenovector. During the experiment, one unhealthy rat from each group was discarded. Two additional aging rats were used to characterize short-term expression of RAd-DsRed. Animals were housed in a temperature-controlled room (22 ± 3 °C) on a 12 : 12 h light/dark cycle with food and water available *ad libitum*. All experiments with animals were done following the Animal Welfare Guidelines of NIH (INIBIOLP's Animal Welfare Assurance No A5647-01). The ethical acceptability of the animal protocols used here have been approved by our institutional IACUC (Protocol # T09-01-2013).

Surgical procedures

Stereotaxic injections

Rats were anesthetized with ketamine hydrochloride (40 mg/kg; ip) plus xylazine (8 mg/kg; im) and placed in a stereotaxic apparatus. Injection in the lateral ventricles were performed placing the tip of a 26G needle fitted to a 10 μL syringe at the following coordinates relative to the bregma: − 0.8 mm anteroposterior, 4.1 mm dorsoventral and ± 1.5 mm mediolateral (Paxinos & Watson, 1998). Rats were injected bilaterally with 8 μL per side of a suspension containing 10^{10} plaque forming units (pfu) of the appropriate vector. On postvector injection day 18, CSF samples were taken as described below and stored at − 70 °C.

CSF collection

Before killing the rats, the CSF was obtained from the great cerebral cistern by puncture as previously documented (Nishida *et al.*, 2011). Briefly, rats were anesthetized as described above and CSF withdrawn with a syringe carrying a 26G needle. With this procedure it was possible to obtain 50–80 μL CSF.

IGF-I assay

IGF-I was extracted from CSF samples (20 μL) by acid-ethanol cryoprecipitation and was radioimmunoassayed using antibody UB2-495 from L. Underwood and J.J. Van Wyk, which is distributed by the Hormone Distribution Program of the National institute of Diabetes and Digestive and Kidney diseases (NIDDK, Bethesda), National Hormone and Pituitary Program. Recombinant human IGF-I (rh IGF-I; Chiron Corp., Emeryville, CA) was used as tracer and the unlabeled ligand. Intra and interassay coefficients of variation were 7.2 and 12.8%, respectively.

Spatial memory assessment and experimental design

We used a previously documented variant of the Barnes maze protocol (Morel *et al.*, 2015). It consists of an elevated (108 cm to the floor) black acrylic circular platform, 122 cm in diameter, containing 20 holes around the periphery. The holes are of uniform diameter (10 cm) and appearance, but only one hole is connected to a black escape box (tunnel). The escape box is 38.7 cm long × 12.1 cm wide × 14.2 cm in depth and it is removable. A white cylindrical starting chamber (25 cm in diameter and 20 cm high) open-ended chamber is used to place the rats on the platform with a random orientation of their bodies. Four proximal visual cues are placed in the room, 50 cm away from the circular platform. The escape hole is numbered as hole 0 for graphical normalized representation purposes, while the remaining holes are numbered 1 to 10 clockwise, and − 1 to − 9 counterclockwise (Fig. 1A). During the entire experiment, hole 0 remained in a fixed position, relative to the cues in order to avoid randomization of the relative position of the escape box. A 90-dB white-noise generator and a white-light 500 W bulb provided the escape stimulus from the platform.

At the beginning of the experiment, the rats were habituated to the task. The habituation routine consists of placing the animals in the starting chamber and the escape box for 180 s each.

Before and after vector injection we used an abbreviated protocol based on 3 days of acquisition trials (AT, two ATs per day), followed by a probe trial (PT) 1 day after the AT series. An AT consists of placing a rat in the starting chamber, located at the center of the platform, for 30 s, the chamber is then raised, the aversive stimuli (bright light and high pitch noise) are switched on and the rat is allowed to freely explore the maze for 60 s. The purpose of ATs is to train the rats on finding the escape hole. A PT is similar to ATs except that the escape box has been removed, its purpose being to assess recent spatial memory retention.

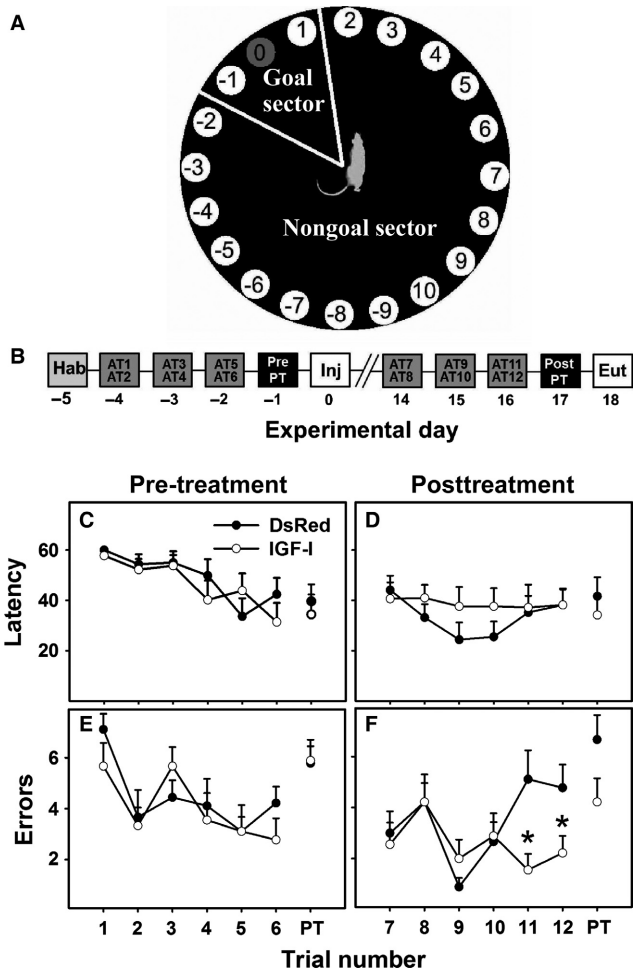

FIG. 1. Effect of IGF-I gene therapy on the performance of old rats in the Barnes Maze. Panel (A) shows the maze from above. It consists of a black acrylic circular platform, 122 cm in diameter, containing 20 holes around the periphery. The holes are of uniform diameter (10 cm) and appearance, but only one hole is connected to a black escape box. Panel (B) depicts the experimental design of the study. Panels (C) and (D) show escape hole latency throughout training and in probe trial before and after treatment, respectively in the DsRed and IGF-I groups. Panels (E) and (F) show the number of errors during training and probe trial before and after treatment, respectively in the same groups. $n = 9$ for all groups. Hab, habituation; AT, acquisition trial; Pre PT, pretreatment probe trial; Inj., vector injection; Post PT, posttreatment probe trial; Eut., euthanasia.

The behavioral performances were recorded using a computer-linked video camera mounted 110 cm above the platform. The video-recorded performances of the subjects were measured using the KINOVEA v0.7.6 (http://www.kinovea.org) software. The behavioral parameters assessed were as follows.

(a)Escape box latency: time (in s) spent by an animal since its release from the starting chamber until it enters the escape box (during an AT) or until the first exploration of the escape hole (during a PT).

(b)Nongoal hole exploration: number of explorations of holes different from the escape one. Each exploration of an incorrect hole is counted as an error, provided that the rat lowers its nose below the plane of the table surface.

(c)Exploration frequency in the goal sector (GS): the sum of the number of explorations for holes − 1, 0, and 1 divided by 3, during a PT.

(d)Exploration frequency in the nongoal sector (NGS): the sum of explorations of the 17 nongoal holes (i.e., all except holes − 1, 0, + 1) divided by 17, in a single PT.

(e)Goal-seeking activity: the sum of explorations for all holes in a PT, divided by 20 (i.e., mean explorations per hole).

(f)Path length: distance (in cm) covered by an animal during a given trial, estimated on the basis of reconstructing the route using the KINOVEA software. This parameter was assessed in pre and postvector injection PT.

(g)Mean velocity (cm/s): is defined as the path length divided by trial duration during acquisition and probe trials. This measurement does not discriminate between activity and inactivity periods. Path length and mean velocity are reference parameters for locomotion performance. These parameters were assessed in PT pre and postvector injection.

Experimental design

The day of vector injection was defined as experimental day 0. Before and after vector injection a full Barnes test, comprising six ATs and a PT, was performed on all rats as diagrammatically illustrated in Fig. 1B. Two DsRed old females, not submitted to the Barnes maze test, were killed 2 days after vector injection for evaluation of DsRed expression.

Brain processing

Animals were placed under deep anesthesia and perfused with phosphate buffered para-formaldehyde 4%, (pH 7.4) fixative. The brains were removed and stored in para-formaldehyde 4%, (pH 7.4) overnight at 4 °C. Brains were kept in cryopreservative solution at − 20 °C until use. For immunohistochemical assessment, brains were cut coronally in 40 μm-thick sections with a vibratome (Leica).

Immunohistochemistry

All immunohistochemical techniques were performed on free-floating sections. For each animal, separate sets of sections were immunohistochemically processed using either a GFAP mouse monoclonal antibody 1 : 500 (Sigma, Saint Louis, MO) or an anti-double cortin (DCX) goat polyclonal antibody 1 : 250 (Santa Cruz Biotech., Dallas, TX). Briefly, after overnight incubation at 4 °C with the primary antibody, sections were incubated with biotinylated horse anti-mouse antiserum (1 : 300, BA-2000; Vector Labs.) or horse anti-goat antiserum (1 : 300, BA-9500, Vector Labs), as appropriate, for 120 min, rinsed and incubated with avidin-biotin-peroxidase complex (1 : 500, PK-6100; Vector ABC Elite Kit) for 90 min and then incubated with 3,3-diamino benzidinetretrahydrochloride. Sections were dehydrated, mounted with Vectamount (Vector) and used for image analysis. Sections immunostained for GFAP were counterstained with cresyl violet (Nissl staining) as described elsewhere (Morel *et al.*, 2015).

Image analysis

In each hippocampal block, one in every six serial sections was selected in order to obtain a set of noncontiguous serial sections spanning the dorsal portion of the hippocampus, which typically comprises about 48 coronal sections, thus yielding eight sets of noncontiguous serial sections (240 μm apart) and is typically located

between coordinates − 2.8 mm and − 4.5 mm relative to the bregma (Paxinos & Watson, 1998). For stereological analysis we used an Olympus BX-51 microscope attached to an Olympus DP70 CCD video camera (Tokyo, Japan).

The volume of the stratum radiatum (SR) and dentate hilus (DH) was assessed on Nissl stained sections with the Cavalieri method (Howard & Reed, 2005). All morphological parameters were assessed bilaterally.

Neuroblast analysis

A stereological assessment of total bilateral migrating neuroblasts, immunoreactive to DCX antibody (DCXir), was performed in the Dentate Gyrus (DG), which includes the hippocampal subgranular zone (SGZ) and granular cell layer (GCL) (Paxinos & Watson, 1998). Neuroblast (DCXir cells) number was assessed as already described (Morel *et al.*, 2015). Due to the low numbers of DCXir neurons in the old rats, the entire DG sections were used as the counting frame, making the area sampling fraction (asf) = 1. The section sampling fraction (ssf) was 1/6. Estimates were based on counting DCXir cell bodies as they came into focus. $n = 6$ animals per group. Branching complexity and process length analysis could not be done for DCXir cells due to insufficient number to achieve statistical validity.

Astroglial cell analysis

The morphologic assessment of GFAP immunoreactive astrocytes (GFAPir) was perfomed in the SR, whose upper limit is the CA1 pyramidal layer, lower limit is Stratum Lacunosum Molecular and the lateral limit is the Stratum Lucidum of the dorsal hippocampus (Paxinos & Watson, 1998). The total number of cells was estimated using a modified version of the optical dissector method (West, 1993). Individual estimates of the total bilateral cell number (n) were calculated according to the following formula: n = RQR.1/ssf.1/asf.1/tsf, where RQR is the sum of counted cells, ssf is the section sampling fraction, asf is the area sampling fraction, and tsf is the thickness sampling fraction. Cells intersecting the exclusion boundaries of the counting frame were not counted. For this study, ssf was equal to 1/6, tsf was equal to 1 and asf was 1/10. $n = 6$ rats for both groups of animals. Counting was performed at 1000× magnification. GFAPir astrocyte number in SR was estimated for every rat.

In order to study branching complexity, GFAPir astrocytes were submitted to Sholl analysis (Sholl, 1953). This technique consists of superimposing a mask with concentric rings distributed at equal distances d (5 μm) centered on a cell soma. The number of process intersections per ring 'i' (an index of branching complexity) was computed and the total length of the processes was estimated by the sum of the i values for each ring multiplied by 5.

For Sholl analysis, images (1000×) of the SR were taken throughout representative coronal sections spanning the SR. In each rat (six per group), 160 astrocytes were randomly chosen. The length of the processes of astrocytes and their branching complexity at every distance from the soma was averaged for every rat and this output data was used for the statistical analysis between groups.

Statistical analysis

Data were compiled and analyzed with the SIGMA PLOT v.11 software (Systat Software, Inc., San Jose, CA, USA). Behavioral and stereological data are presented as mean ± SEM. Acquisition trial comparisons between groups were assessed using repeated-measures analysis of the variance (RM-ANOVA). When the RM-ANOVA was significant, the Holm–Sidak method was chosen as a post hoc test. Differences were considered significant when $P < 0.05$. Additionally, some parameters of probe trials were analyzed using unpaired Student's t-test.

Unpaired Student's t test was also used for statistical analysis of stereological data and CSF IGF-I levels with the SIGMA PLOT 11 software.

Results

Cognitive changes

Latency to escape box

This parameter is a measure of learning. Before treatment, escape hole latency fell significantly at comparable rates (Two way RM-ANOVA: treatment factor: DF = 1; $F = 0.0419$; $P = 0.840$; trial factor: DF = 13; $F = 3.654$; $P < 0.001$; interaction treatment × trial: DF = 13; $F = 1.068$; $P = 0.389$) in both the DsRed and IGF-I groups, from AT1 to AT6 and was also similar in the pretreatment PT (Fig. 1C).

The latency performance after treatment (AT7) began at better levels than at pretreatment (AT1) in both groups (Holm-Sidak post hoc test $P = 0.008$) and tended to be lower in the DsRed than in the IGF-I group but the trend did not reach significance (Fig. 1D). Posttreatment PT results were similar for both groups.

Errors to escape box

In the pretreatment AT series, nongoal hole exploration (i.e., errors) decreased significantly throughout the training process. (Two way RM-ANOVA: treatment factor: DF = 1; $F = 1.956$; $P = 0.181$; trial factor: DF = 13; $F = 3.837$; $P < 0.001$; interaction treatment × trial: DF = 13; $F = 1.235$; $P = 0.257$) (Fig. 1E). The number of posttreatment errors varied rather erratically from AT7 to AT12 in the DsRed group, but remained low in the IGF-I group, becoming significantly lower at AT11 and AT12 (Holm-Sidak pos-hoc test $P = 0.004$ and $P = 0.038$, respectively) than the corresponding control points. (Fig. 1F).

Hole exploration frequency

As expected, hole exploration frequency showed overlapping bell-shaped distributions around hole 0 in the pretreatment PT (experimental day − 1) (Fig. 2A). After treatment, exploration frequency of the goal hole (hole 0) in the IGF-I group was significantly higher than in the DsRed counterparts (Mann–Whitney test $P = 0.015$), whereas, the DsRed and IGF-I group showed comparable levels of exploratory frequency for almost every corresponding pair of non-goal holes (Fig. 2B).

Goal-seeking activity declined significantly after treatment in both groups (Paired Student's t-test for each Pretreatment vs. Posttreatment pairs; $P < 0.05$). GS exploration frequency did not change after treatment (Fig. 3).

Path length and mean velocity

Insulin-like growth factor-I gene therapy did not have a significant (Student's t-test, $P > 0.40$) impact on either path length or mean velocity (data not shown).

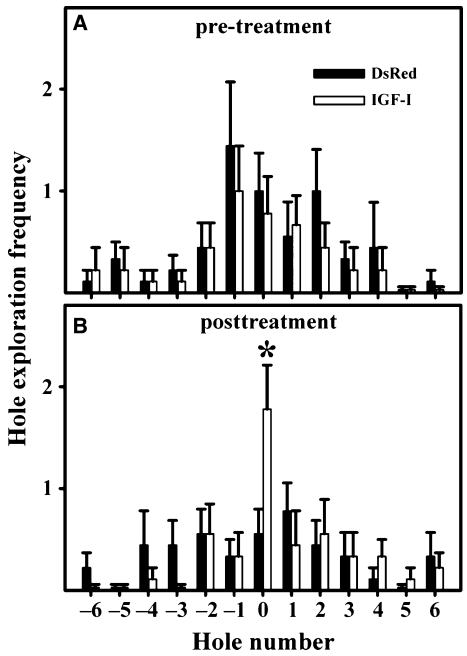

FIG. 2. Effect of IGF-I gene therapy on hole exploration frequency. At pretreatment (A) both groups showed a similar bell-shaped distribution of frequencies around hole #0. After treatment (B) the exploration frequency of the IGF-I group for the escape hole was significantly higher than that of the DsRed counterparts. Exploration frequency in the other holes remained generally similar for DsRed vs. IGF-I rats for the equivalent holes in the platform. Number of IGF-I and DsRed rats was 9 for both. Other details are as in Fig. 1.

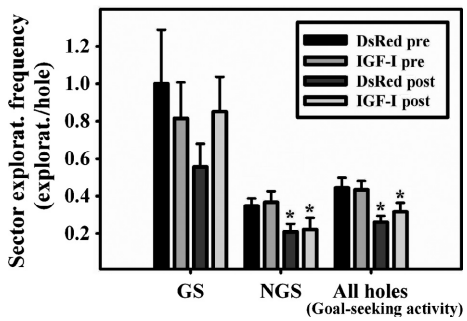

FIG. 3. Effect of IGF-I gene therapy on sector exploration frequency and goal-seeking activity. Even though IGF-I gene therapy prevented the fall in GS exploratory frequency after treatment to a greater extent than DsRed vector injection, this difference did not reach significance. GS, goal sector; NGS, nongoal sector. All holes, the 20 holes of the Barnes platform taken as a single sector. The mean exploration frequency for all holes (20) represents the goal-seeking activity of the corresponding experimental group. Comparisons were made versus the corresponding pretreatment counterparts with Student's paired *t*-test. *$P < 0.05$: $n = 9$ in all groups.

Transgene expression

Two days after RAd-DsRed injection there was a strong expression of DsRed in the ependymal cell layer of all cerebral ventricles (Figs 4a–d). Eighteen days after vector injection transgene expression in the ependymal cell layer was weaker but still observable (Figs 4e–h). At experimental day 18, CSF levels of IGF-I were much higher (Student's *t*-test, $P < 0.001$) in the treated than in the DsRed group (Fig. 4i).

Morphologic changes in the dorsal hippocampus

The volume of the SR and DH showed no significant differences (Student's *t*-test, $P = 0.148$ and Mann–Whitney test, $P = 0.686$, respectively) between the IGF-I and DsRed group (Fig. 5).

The IGF-I group showed a significant increase (Student's *t*-test $P = 0.046$) in the number of DCXir cells (neuroblasts) in the DG as compared to the DsRed group (Figs 6A–C) while the number of GFAPir (astroglial) cells in the SR was significantly lower (Student's *t*-test $P = 0.025$) in the IGF-I than in the DsRed rats (Figs 6D–H).

We found a significant increase in branching complexity at 5 and 10 μm from the soma (Student's *t*-test $P = 0.010$ and $P = 0.029$ for 5 and 10 μm, respectively). Additionally, intersections at distances 15 and 20 μm showed a clear trend toward greater branching for IGF-I (Student's *t*-test $P = 0.075$ and $P = 0.083$ for 15 and 20 μm, respectively).

A trend toward an increase in the mean length of astrocyte processes was observed in the IGF-I versus the DsRed group (Student's *t*-test $P = 0.058$) (Fig. 7).

Discussion

Spatial memory declines with age in rats as revealed by various tests of spatial learning and memory such as the radial arm maze (de Toledo-Morrell *et al.*, 1984), the Morris Water Maze (MWM; Morris, 1984) and the Barnes maze (Barnes, 1979; Morel *et al.*, 2015). The hippocampus of the rat exhibits complex, region selective changes in its functional organization during aging (Barnes, 1998) but no significant neuron loss (Rapp & Gallagher, 1996). Hippocampal neurogenesis is important for certain types of memory and falls significantly in aged rats (Lichtenwalner *et al.*, 2001; Morel *et al.*, 2015). Age-related decline in hippocampal neurogenesis may be linked in part, to the well-established reduction in serum and brain IGF-I levels in aged rats (Sonntag *et al.*, 1980). Besides its neurogenic activity, IGF-I exerts a multifaceted modulatory action on brain function throughout lifespan (Fernandez & Torres-Alemán, 2012). We chose the ependymal route for IGF-I gene delivery to the brain based on the fact that most of the peptide used by the CNS comes from the circulation (Carro *et al.*, 2000, 2006b), and is actively transported through the choroid plexus to the CSF, from where the molecule reaches specific areas of the brain by unknown mechanisms (Guan *et al.*, 1996; Carro *et al.*, 2000). Therefore, the ependymal route appears to be a suitable strategy to perform IGF-I-gene delivery to the brain. We chose an adenoviral vector for ICV gene therapy based on the fact that these vectors are highly selective for ependymal cells, which are efficiently transduced by RAd-IGF-I and substantially increase IGF-I levels in CSF (Hereñú *et al.*, 2009). Our data confirm that adenovectors efficiently transduce the ependymal cell layer and that our IGF-I adenovector increases CSF levels of IGF-I even 18 days after injection (Fig. 4).

Clearly, transgenic IGF-I released to the CSF will act on many brain structures. We chose to study its effects on hippocampal morphology because this is a key brain region for spatial memory formation and initial storage (Restivo *et al.*, 2009). Within the hippocampus, we focused our stereological assessment on immature neurons and astroglial cells in the DG and in the SR, respectively, two regions vulnerable to degeneration in AD patients (West *et al.*, 1994).

In most rodent studies, spatial memory has been assessed using the MWM. However, a potential disadvantage of the MWM in aging studies is that it requires a substantial degree of physical

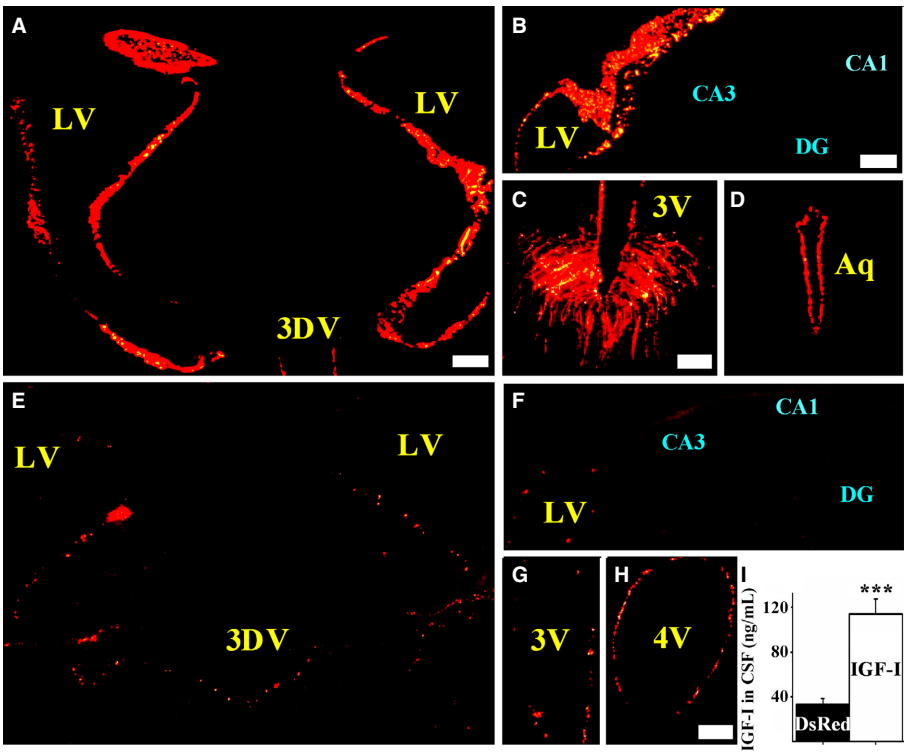

FIG. 4. Transgene expression and IGF-I levels in the CSF of DsRed and IGF-I rats. Panels (A–D) show expression levels (red fluorescence) of DsRed in the ependymal layer of old rats 2 days after RAd-DsRed vector injection. Panels (E–H) show DsRed expression at the end of the experiment (experimental day 18). Panel (I) shows CSF IGF-I levels on experimental day 18 in DsRed and IGF-I animals. In panel (i), *n* was 5 and 4 for the DsRed and IGF-I groups, respectively. LV, lateral ventricle; 3V, third ventricle; 3DV, third ventricle dorsal; Aq, aqueduct; 4V, fourth ventricle; CA1, CA3 and DG, refer to hippocampal regions. Scale bar for panel (A) = 200 μm which also applies to panel (E); scale bar for panel (B) = 150 μm which also applies to panel (F); Scale bar for panel (C) = 100 μm which also applies to panel (D); Scale bar for panel (G) = 50 μm which also applies to panel (H). *** $P < 0.001$.

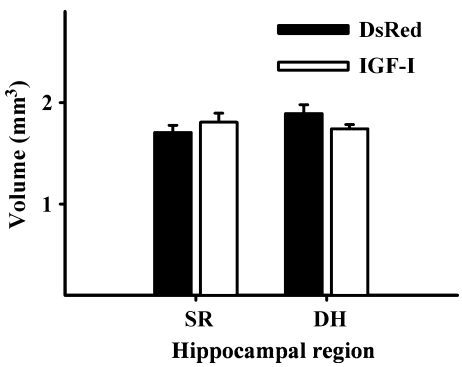

FIG. 5. Effect of IGF-I gene therapy on the volume of stratum radiatum (SR) and dentate hilus (DH). The number of specimens measured was 4 for both the DsRed and IGF-I groups. No significant differences were detected.

fitness. Therefore, we chose the less physically demanding Barnes maze for assessing spatial memory in aging rats. In both tests, rats learn to use spatial cues to guide them to a hidden platform or tunnel. While the MWM involves immersion in water, a stimulus that provokes considerable corticosterone and corticotropin release (Sternberg *et al.*, 1992), in the Barnes maze animals are placed on an open platform for them to walk in search of the escape hole.

Insulin-like growth factor-I gene therapy reduced the number of errors made by the old rats ATs 11 and 12 learning sessions as compared with their placebo counterparts. It is important to point out that *n* values were low. Had they been higher additional significant differences may have emerged at other time points.

Nevertheless, the most remarkable effect of the treatment was on hole exploration where the treatment markedly increased exploratory activity at the escape hole as compared to DsRed controls. As the exploration frequency of the other holes by IGF-I animals remained generally similar to that of DsRed counterparts, the restorative action of transgenic IGF-I on spatial memory seems to have been highly specific as the treatment increased the accuracy of the animals to remember the escape hole without significantly affecting other mnemonic parameters. We have previously shown that the accuracy to remember the escape hole in the Barnes maze declines with age in rats, a change that is paralleled by an age-related reduction in the numbers of DCXir neurons in the DG (Morel *et al.*, 2015). Importantly, it has been documented that in 28 months old male Brown Norway X Fischer 344 rats, there is a significant reduction in the number of newly generated cells in the DG as well as a 60% reduction in the differentiation of newborn cells into neurons (Lichtenwalner *et al.*, 2001). Furthermore, the same study demonstrated that ICV administration of IGF-I peptide to the old animals significantly restored hippocampal neurogenesis through an approximately threefold increase in neuronal production, without having any effect on progenitor differentiation to neurons or on survival of newborn cells. In another study Åberg *et al.* (2000) documented that peripheral administration of IGF-I peptide to young hypophysectomized female Sprague Dawley rats stimulated neurogenesis (but not astrogenesis) in the DG as well as differentiation of newborn progenitors to neurons. The treatment also increased newborn cell survival. Therefore it seems that while peripheral and central delivery of IGF-I peptide have a stimulatory effect on DG neurogenesis, the effects of the treatments on newborn cell differentiation and survival are

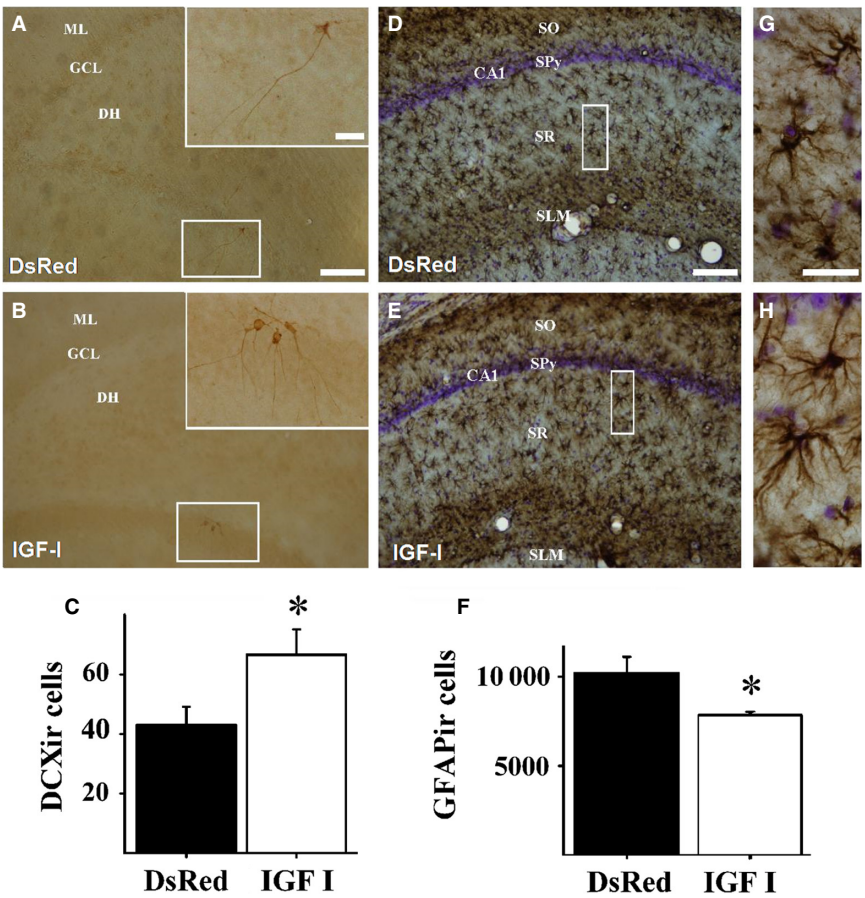

FIG. 6. DCX and GFAP expression in the dorsal hippocampus. Coronal sections of representative animals from the DsRed and IGF-I groups showing DCXir neurons (A, B), and GFAPir cells (D, E). Insets (G) and (H) to the right of (D) and (E), represent magnified views of framed areas in the respective images. Panels (C) and (F) show plots representing DCXir and GFAPir cell numbers, respectively, in the DG and SR of control and experimental rats. Number of DsRed and IGF-I hippocampi was 6 for both. Abbreviations, ML, molecular layer, GCL, granular cell layer, DH, dentate hilus; SO, stratum oriens; Spy, stratum pyramidale; CA1, cornus ammonis 1; SR, stratum radiatum; SLM, stratum lacunosum moleculare. Scale bars, 100 μm; insets, 20 μm. * $P < 0.05$.

dissimilar. These differential effects might be also accounted for by the marked age difference of the animals used.

Using a place discrimination test in the MWM, Markowska *et al.* (1998) showed that IGF-I administered via repeated ventricular osmotic mini pump implants (for 28 days) to 32 months old rats significantly increased the number of crossings over a hidden platform in the probe trials as compared to nontreated counterparts. This finding is consistent with our results as in the MWM, the platform crossings is a measure of the accuracy with which the animals remember the localization of the platform and in this regard is equivalent to the measure of exploration frequency of the escape hole in the Barnes maze.

After treatment, average goal-seeking activity, which reflects the motivation of rats to search for the target hole, fell significantly in both experimental groups. The same was true for NGS exploration frequency in both groups. This may be due in part to the fact that at the second PT, where the rats were exposed to the Barnes maze environment, it was less novel to the animals than the first time (i.e. before the treatment). IGF-I gene therapy prevented the fall in GS exploratory frequency after treatment to a greater extent than DsRed vector injection did, an observation that suggests a selective enhancing action of IGF-I on goal-associated memory.

In rats, hippocampal astrogliosis increases with age, being already elevated in mid-life (13 months). The phenomenon is characterized by a marked reactive hypertrophy of astrocytes and a moderate increase in the numbers of these cells (Lindsey *et al.*, 1979). There is proof that age-related astrocyte activation is disruptive to neuronal function (Rozovsky *et al.*, 2005).

Our finding that ICV gene therapy reduces the number of astrocytes (GFAPir cells) in the hippocampal SR region suggests that this peptide has the ability to reverse some of the age-related gliosis in the hippocampus. This is consistent with the fact that IGF-I exerts a protective action on astrocytes, contributing to the resilience of these glial cells against oxidative stress (Genis *et al.*, 2014).

We have reported an age-related reduction in the length and complexity of hippocampal astrocyte processes in female rats (Morel *et al.*, 2015). To our knowledge, this is the first report that administration of IGF-I *in vivo* restores astrocyte branching in old rats. We are unaware of any reported effects of IGF-I on astrocyte branching. As mentioned above, IGF-I is known to protect astrocytes against oxidative stress (Genis *et al.*, 2014) and is also known not to induce astrogenesis in the adult rat hippocampus (Åberg *et al.*, 2000).

Conclusions

It is well-established that IGF-I has pleoitropic actions on the CNS including neurogenesis and neuroprotection. The present results show that overexpression of the peptide in the aging rat brain is able

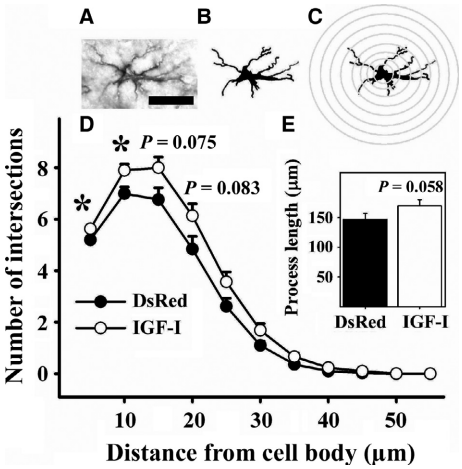

FIG. 7. Effect of IGF-I treatment on the length and branching complexity of glial processes in the stratum radiatum. In the upper row, panel (A) shows the micrograph of a single astrocyte, panel (B) represents an astrocyte silhouette. Panel (C) shows the result of superimposing a mask with concentric rings distributed at equal distances and centered on the GFAP immunoreactive soma of the cell. The number of process intersections *i* per ring was computed as branching complexity. Asterisks represent significant differences between IGF-I rats and the corresponding DsRed controls for the indicated points. (D) The inset (E) shows the average length of astrocyte processes in DsRed and IGF-I groups in the SR. The length of the processes was estimated by the sum of the *i* values for each ring multiplied by 5. The number of hippocampi assessed was 6 for each age group. Scale bar: 20 μm.

to improve the accuracy of spatial memory, partially restores neurogenesis in the DG and improves astrocyte branching in the SR. This restorative effect was achieved after a relatively short exposure of the CNS to transgenic IGF-I (18 days). It seems therefore possible that a longer exposure of the brain to the peptide could affect additional restorative actions on spatial memory in old rodents.

Acknowledgements

The authors are indebted to Ms. Yolanda E. Sosa and Mr. Oscar Vercellini for technical and to Drs. Jorge Lopez-Camelo and Fernando Poletta, for assistance with the statistical analysis. GRM, PCR and RGG are career researchers of the Argentine Research Council (CONICET). JP is a recipient of a CONICET doctoral fellowship and was supported by a German-Argentine (Ale-Arg) travel fellowship. This work was supported by grants #PICT11-1273 and #PICT13-1590 from the Argentine Agency for the Promotion of Science and Technology and grant PIP0597 from CONICET to RGG. TFO is supported by the DFG Center for Nanoscale Microscopy and Molecular Physiology of the Brain.

Abbreviations

AT, acquisition trial; CSF, cerebrospinal fluid; DCX, doublecourtin; DG, dentate gyrus; DH, dentate hilus; GCL, granular cell layer; GFAP, glial fibrillary acidic protein; GS, goal sector; ICV, intracerebroventricular; IGF-I, insulin-like growth factor I; mCMV, mouse cytomegalovirus; ML, molecular layer; MWM, Morris water maze; NGS, nongoal Sector; PT, probe trial; RAd, recombinant adenoviral vector; SR, stratum radiatum.

References

Åberg, M.A., Åberg, N.D., Hedbacker, H., Oscarsson, J. & Eriksson, P.S. (2000) Peripheral infusion of IGF-I selectively induces neurogenesis in the adult rat hippocampus. *J. Neurosci.*, **20**, 2896–2903.

Barnes, C.A. (1979) Memory deficits associated with senescence: a neurophysiological and behavioral study in the rat. *J. Comp. Physiol. Psych.*, **93**, 74–104.

Barnes, C.A. (1998) Spatial cognition and functional alterations of aged rat hippocampus. In Wang, E. & Snyder, D.S. (Eds), *Handbook of the Aging Brain*. Academic Press, New York, pp. 51–66.

Beilharz, E.J., Russo, V.C., Butler, G., Baker, N.L., Connor, B., Sirimanne, E.S., Dragunow, M., Werther, G.A. *et al.* (1998) Co-ordinated and cellular specific induction of the components of the IGF/IGFBP axis in the rat brain following hypoxic-ischemic injury. *Brain Res. Mol. Brain Res.*, **59**, 119–134.

Breese, C.R., D'Costa, A., Rollins, Y.D., Adams, C., Booze, R.M., Sonntag, W.E. & Leonard, S. (1996) Expression of insulin-like growth factor-1 (IGF-I) and IGF-binding protein 2(IGF-BP2) in the hippocampus following cytotoxic lesion of the dentate gyrus. *J. Comp. Neurol.*, **369**, 388–404.

Carro, E., Nunez, A., Busiguina, S. & Torres-Aleman, I. (2000) Circulating insulin-like growth factor I mediates effects of exercise on the brain. *J. Neurosci.*, **20**, 2926–2933.

Carro, E., Trejo, J.L., Gerber, A., Loetscher, H., Torrado, J., Metzger, F. & Torres-Aleman, I. (2006a) Therapeutic actions of insulin-like growth factor I on APP/PS2 mice with severe brain amyloidosis. *Neurobiol. Aging*, **27**, 1250–1257.

Carro, E., Trejo, J.L., Spuch, C., Bohl, D., Heard, J.M. & Torres-Aleman, I. (2006b) Blockade of the insulin-like growth factor I receptor in the choroid plexus originates Alzheimer's-like neuropathology in rodents: new cues into the human disease?. *Neurobiol. Aging*, **27**, 1618–1631.

Dore, S., Kar, S. & Quirion, R. (1997) Insulin-like growth factor-1 protects and rescues hippocampal neurons against amyloid- and amylin-induced toxicity. *Proc. Natl. Acad. Sci. USA*, **94**, 4772–4777.

Fernandez, A.M. & Torres-Alemán, I. (2012) The many faces of insulin-like peptide signalling in the brain. *Nat. Rev. Neurosci.*, **13**, 225–239.

Genis, L., Dávila, D., Fernandez, S., Pozo-Rodrigálvarez, A., Martínez-Murillo, R. & TorresAleman, I. (2014) Astrocytes require insulin-like growth factor I to protect neurons against oxidative injury. *F1000Res*, **3**, 28. doi:10.12688/f1000research.3-28.v2.

Guan, J., Skinner, S.J., Beilharz, E.J., Hua, K.M., Hodgkinson, S., Gluckman, P.D. & Williams, C.E. (1996) The movement of IGF-1 into the brain parenchyma after hypoxic–ischaemic injury. *NeuroReport*, **7**, 632–636.

Hereñú, C.B., Cristina, C., Rimoldi, O.J., Becú-Villalobos, D., Cambiaggi, V., Portiansky, E.L. & Goya, R.G. (2007) Restorative effect of Insulin-like Growth Factor-I gene therapy in the hypothalamus of senile rats with dopaminergic dysfunction. *Gene Ther.*, **14**, 237–245.

Hereñú, C.B., Sonntag, W.E., Morel, G.R., Portiansky, E.L. & Goya, R.G. (2009) The ependymal route for insulin like growth factor-1 gene therapy in the brain. *Neuroscience*, **163**, 442–447.

Howard, C.V. & Reed, M.G. (2005) *Unbiased Stereology*, 2nd Edn. Garland Science/BIOS Scientific Publishers, Oxon, UK.

Li, X.S., Williams, M. & Bartlett, W.P. (1998) Induction of IGF-1 mRNA expression following traumatic injury to the postnatal brain. *Brain Res. Mol. Brain Res.*, **57**, 92–96.

Lichtenwalner, R.J., Forbes, M.E., Bennett, S.A., Lynch, C.D., Sonntag, W.E. & Riddle, D.R. (2001) Intracerebroventricular infusion of insulin-like growth factor-I ameliorates the age-related decline in hippocampal neurogenesis. *Neuroscience*, **107**, 603–613.

Lindsey, J.D., Landfield, P.W. & Lynch, G.J. (1979) Early onset and topographical distribution of hypertrophied astrocytes in hippocampus of aging rats: a quantitative study. *J. Gerontol.*, **34**, 661–671.

Markowska, A.L., Mooney, M. & Sonntag, W.E. (1998) Insulin-like growth factor-1 ameliorates age-related behavioral deficits. *Neuroscience*, **87**, 559–569.

Morel, G.R., Andersen, T., Pardo, J., Zuccolilli, G.O., Cambiaggi, V., Hereñú, C.B. & Goya, R.G. (2015) Cognitive impairment and morphological changes in the dorsal hippocampus of very old female rats. *Neuroscience*, **303**, 189–199.

Morris, R. (1984) Developments of a water-maze procedure for studying spatial learning in the rat. *J. Neurosci. Meth.*, **11**, 47–60.

Nishida, F., Morel, G.R., Hereñú, C.B., Schwerdt, J.I., Goya, R.G. & Portiansky, E.L. (2011) Restorative effect of intracerebroventricular insulin-like growth factor-I gene therapy on motor performance in aging rats. *Neuroscience*, **177**, 195–206.

Paxinos, G. & Watson, C. (1998) *The Rat Brain in Stereotaxic Coordinates*. Academic Press, San Diego.

Rapp, P.R. & Gallagher, M. (1996) Preserved neuron number in the hippocampus of aged rats with spatial learning deficits. *Proc. Natl. Acad. Sci. USA*, **93**, 9926–9930.

Ravindranath, V., Dang, H.M., Goya, R.G., Mansour, H., Nimgaonkar, V.L., Russell, V.A. & Xin, Y. (2015) Regional research priorities in brain and nervous system disorders. *Nature*, **527**, S198–S206.

Restivo, L., Vetere, G., Bontempi, B. & Ammassari-Teule, M. (2009) The formation of recent and remote memory is associated with time-dependent formation of dendritic spines in the hippocampus and anterior cingulate cortex. *J. Neurosci.*, **29**, 8206–8214.

Rodriguez, S.S., Schwerdt, J.I., Barbeito, C.G., Flamini, A.M., Han, Y., Bohn, M.C. & Goya, R.G. (2013) Hypothalamic insulin-like growth factor-I gene therapy prolongs estral cyclicity and protects ovarian structure in middle-aged female rats. *Endocrinology*, **154**, 2166–2173.

Rozovsky, I., Wei, M., Morgan, T.E. & Finch, C.E. (2005) Reversible age impairments in neurite outgrowth by manipulations of astrocytic GFAP. *Neurobiol. Aging*, **26**, 705–715.

Sholl, D.A. (1953) Dendritic organization in the neurons of the visual and motor cortices of the cat. *J. Anat.*, **87**, 387–406.

Sonntag, W.E., Steger, R.W., Forman, L.J. & Meites, J. (1980) Decreased pulsatile release of growth hormone in old male rats. *Endocrinology*, **107**, 1875–1879.

Sternberg, E.M., Glowa, J.R., Smith, M.A., Calogero, A.E., Listwak, S.J., Aksentijevich, S., Chrousos, G.P., Wilder, R.L. *et al.* (1992) Corticotropin releasing hormone related behavioral and neuroendocrine responses to stress in Lewis and Fischer rats. *Brain Res.*, **570**, 54–60.

de Toledo-Morrell, L., Morrell, F. & Fleming, S. (1984) Age-dependent deficits in spatial memory are related to impaired hippocampal kindling. *Behav. Neurosci.*, **98**, 902–907.

Walter, H.J., Berry, M., Hill, D.J. & Logan, A. (1997) Spatial and temporal changes within wounds in the insulin-like growth factor (IGF) axis indicate autocrine/paracrine actions of of the rat brain. *Endocrinology*, **138**, 3024–3034.

West, M.J. (1993) New stereological methods for counting neurons. *Neurobiol. Aging*, **14**, 275–285.

West, M., Coleman, P., Flood, D. & Troncoso, J. (1994) Differences in the pattern of hippocampal neuronal loss in normal ageing and Alzheimer's disease. *Lancet*, **344**, 769–772.

Yao, D.L., West, N.R., Bondy, C.A., Brenner, M., Hudson, L.D., Zhou, J., Collins, G.H. & Webster, H.D. (1995) Cryogenic spinal cord injury induces astrocytic gene expression of insulin-like growth factor I and insulin-like growth factor binding protein 2 during myelin regeneration. *J. Neurosci. Res.*, **40**, 647–659.